https://doi.org/10.5194/wes-2025-164
Preprint. Discussion started: 29 September 2025

eawe european academy of wind energy
Open Access WIND ENERGY SCIENCE DISCUSSIONS

Investigation on the Impacts of Smart Curtailment for Bat Fatality Mitigation in Alberta

Anastasiia Sobchenko[1], Ian Maynard[1], Ryan Kilpatrick[1], and Keelia LaFreniere[1]

[1]Natural Resources Canada, CanmetENERGY–Ottawa, Ottawa, K1A 1M1, Canada

Correspondence: Anastasiia Sobchenko (anastasiia.sobchenko@nrcan-rncan.gc.ca), Ian Maynard (ian.maynard@nrcan-rncan.gc.ca)

Abstract. As wind energy continues to expand in Canada, it is increasingly important to balance power generation with wildlife conservation. For migratory bat species, the risk of interactions with wind turbines varies throughout the year. In response to environmental conditions, curtailing turbine operation during periods of higher risk has been shown to reduce bat fatalities. This study models seasonal turbine curtailment scenarios across wind farms in the Canadian province of Alberta to estimate the resulting energy and economic impacts. High-resolution weather data were used to reconstruct complete wind speed records and simulate turbine output. The modeled power output was closely aligned with real production data reported by the province's energy operator. Results indicate that curtailment outcomes vary significantly depending on wind speed thresholds, seasonal wind conditions, and curtailment duration. Across all scenarios, smart curtailment reduced energy and financial losses by 20–40% compared to blanket curtailment, highlighting the benefits of using meteorological and behavioral triggers. These findings provide practical insights for minimizing energy loss while supporting conservation goals.

1 Introduction

As nations work toward net-zero emissions, renewable energy expansion is crucial. According to the International Energy Agency, global renewable electricity capacity is expected to grow by 5,500 GW by 2030, reaching nearly 940 GW of new additions annually – 70% more than the current record. Solar and wind are projected to account for 95% of this growth due to their increasing cost-competitiveness (International Energy Agency, 2024). However, the expansion of wind turbines poses ecological risks, particularly to migratory bat populations, which are vulnerable to collisions with turbine blades that interfere with their flight paths. In addition to turbine-related fatalities, migratory bat populations are already declining due to habitat loss and white-nose syndrome (Frick et al., 2023).

This study models the impact of curtailment scenarios on wind power generation and revenue loss for Alberta, which had the largest installed wind capacity of any province in Canada by the end of 2024 (approximately 5.7 GW), contributing to Canada's total energy capacity (wind, solar, and storage) of about 24 GW (International Energy Agency, 2024; Canadian Renewable Energy Association, 2024). Using high-resolution weather data and turbine-specific characteristics, CanmetEnergy-Ottawa (CE-O) simulated wind power output at several wind farms and compared modeled results to observed production data. CE-O

https://doi.org/10.5194/wes-2025-164
Preprint. Discussion started: 29 September 2025

eawe european academy of wind energy
Open Access WIND ENERGY SCIENCE DISCUSSIONS

then evaluated energy and financial losses under multiple curtailment strategies, including variations in cut-in wind speed and curtailment duration, to assess trade-offs between energy efficiency and bat conservation outcomes.

2 Background

The growing scale of wind energy presents increasing risks to migratory bat populations, which are already in decline due to multiple stressors including habitat loss, white-nose syndrome, and turbine collisions. As of January 2024, several species such as the Eastern Red Bat, Hoary Bat, and Silver-haired Bat have been classified as endangered in Ontario (Ontario Ministry of the Environment, Conservation and Parks, 2025). These species have now been added to the list of at-risk bats, which already includes the Little Brown Myotis, Northern Myotis, and Tricolored Bat (Ontario Ministry of the Environment, Conservation and Parks, 2024). As wind energy continues to expand globally, its ecological impacts, particularly on wildlife, have become a growing focus among policymakers and researchers (Frick et al., 2023; Maclaurin et al., 2022).

One commonly used mitigation approach involves increasing the turbine cut-in wind speed during periods of high bat activity to reduce collision risk. In Ontario, the Ministry of Natural Resources (MNRF) requires wind farms that exceed ten bat fatalities per turbine annually to increase the turbine cut-in wind speed to 5.5 m/s from sunset to sunrise between July 15 and September 30 for the life of the project (Ontario Ministry of Natural Resources and Forestry, 2011). An alternative method of curtailment called smart curtailment uses meteorological-based triggers for targeted turbine shutdowns, reducing energy losses while still mitigating bat fatalities (Maclaurin et al., 2022). These triggers are typically based on atmospheric conditions such as wind speed, temperature, and precipitation. In this study, CE-O implemented a curtailment framework that increased the turbine cut-in wind speed in 0.5 m/s increments from 5.5 m/s to 8.0 m/s, and only activated curtailment when the temperature exceeded 9.5 °C and there was no rainfall, as bats have been observed to be significantly less active in colder or rainy conditions (Maclaurin et al., 2022). However, different versions of smart curtailment exist and may incorporate other environmental criteria such as humidity, cloud cover, or species-specific activity patterns, to tailor curtailment more precisely to local conditions.

Previous efforts by CE-O assessed the economic impacts of the blanket curtailment regime, applying a 5.5 m/s cut-in wind speed from July 15 to September 30, across all wind farms operating in Ontario (Thurber et al., 2023).

To analyze the potential impacts of bat mitigation measures on Alberta wind farms, CE-O modeled two curtailment strategies: blanket curtailment and smart curtailment. Additionally, CE-O considered two seasonal windows that reflect different levels of bat activity: a longer curtailment period from July 15 to September 30, and a shorter period covering peak activity from August 1 to September 10 (Alberta Environment and Sustainable Resource Development, 2013). These combinations resulted in four distinct scenarios: Full Season – Blanket, Full Season – Smart, Peak Season – Blanket, and Peak Season – Smart, as shown in Table 1. “Full Season – Blanket” refers to blanket curtailment applied from July 15 to September 30, while “Full Season – Smart” indicates smart curtailment applied over the same period. Similarly, “Peak Season – Blanket” applies blanket curtailment during a shorter window from August 1 to September 10, and “Peak Season – Smart” refers to smart curtailment during that same shortened period. This structure allowed for evaluation of different curtailment strategies,

https://doi.org/10.5194/wes-2025-164
Preprint. Discussion started: 29 September 2025

eawe european academy of wind energy
Open Access WIND ENERGY SCIENCE DISCUSSIONS

curtailment periods, and turbine cut-in wind speed thresholds on wind energy production and economic performance during the bat migration season.

Table 1. Scenarios with seasonal, temporal, and meteorological constraints.

Scenario category	Full season blanket	Full season smart	Peak season blanket	Peak season smart
Seasonal window	15 July–30 September	15 July–30 September	1 August–10 September	1 August–10 September
Temporal window	1 h before sunset to 1 h after sunrise	1 h before sunset to 1 h after sunrise	Sunset to sunrise	Sunset to sunrise
Cut-in speed	5.5–8 m s^{-1}	5.5–8 m s^{-1}	5.5–8 m s^{-1}	5.5–8 m s^{-1}
Temperature filter	—	$> 9.5\,^{\circ}C$	—	$> 9.5\,^{\circ}C$
Precipitation filter	—	< 1 mm h^{-1}	—	< 1 mm h^{-1}

3 Methodology

For this analysis, CE-O selected 13 wind farms across Alberta based on the availability of consistent, high-quality meteorological and production data. All selected sites were fully operational before 2020, ensuring that the dataset represented stable, long-term performance. Importantly, complete information was available for each wind farm, including the turbine model, number of installed turbines, total capacity, hub height, and the manufacturer's power curves. Table 2 summarizes the selected wind farms and their respective information.

https://doi.org/10.5194/wes-2025-164
Preprint. Discussion started: 29 September 2025

eawe european academy of wind energy
Open Access WIND ENERGY SCIENCE DISCUSSIONS

Table 2. Wind farms selected for the analysis.

No.	Farm name	Latitude	Longitude	Turbine model	No. of turbines	Total capacity (MW)	Hub height (m)
1	Ardenville	49.55	-113.43	V90 3000	23	69	80
2	ARM2262 Castle River	49.50	-114.05	V47 660	60	39	50
3	Blackspring Ridge	50.12	-112.89	V100 1800	166	299	80
4	Blue Trail Wind	49.67	-113.49	V90 3000	22	66	80
5	Enel Alberta Castle Rock	49.58	-114.00	E70 2300	33	77	65
6	Enmax Taber	49.74	-111.97	E70 2300	37	81	85
7	Ghost Pine	51.90	-113.36	GE1.5 SLE	51	81.6	80
8	Halkirk Wind Power Facility	52.26	-112.06	V90 1800	83	150	80
9	Kettles Hill Wind	49.51	-113.81	V80 1800	35	63	80
10	Magrath	49.39	-112.95	GE1.5 SLE	20	30	105
11	Oldman 2 Wind Farm	49.57	-113.85	SWT23 101	20	46	80
12	Suncor Chin Chute	49.68	-112.32	GE1.5 SLE	20	30	105
13	Summerview 1	49.61	-113.78	V80 1800	38	66	70

3.1 Selecting a data source

To identify the locations of wind farms across Alberta, CE-O used Natural Resources Canada's Canadian Wind Turbine Database (CWTDB), a comprehensive and up-to-date resource for tracking wind turbine installations (Natural Resources Canada, 2024). For weather data, CE-O selected datasets from Environment and Climate Change Canada (ECCC), which provides high-resolution, measured hourly meteorological observations (Environment and Climate Change Canada, 2024). These data, collected from ECCC-operated weather stations, offer reliable insights into local atmospheric conditions relevant for wind energy analysis.

ECCC data demonstrated strong alignment with operational wind power output data from the Alberta Electric System Operator (AESO), making it a suitable choice for estimating site-specific meteorological conditions (Alberta Electric System Operator, 2024). For this analysis, CE-O used data from the nearest ECCC weather stations to each Alberta wind farm, including wind speed, temperature, and precipitation records for the years 2020 to 2023. These years were selected to capture recent wind patterns and ensure consistency across all wind farms in the study.

3.2 Filling data gaps

While the ECCC data provided high-resolution and accurate measurements, some weather station records were incomplete, with gaps totaling up to 570 hours per year at certain locations. To address this, CE-O first identified the three closest ECCC

https://doi.org/10.5194/wes-2025-164
Preprint. Discussion started: 29 September 2025

eawe european academy of wind energy
Open Access WIND ENERGY SCIENCE DISCUSSIONS

weather stations to each wind farm and selected the one with the most complete dataset as the primary station. Then data gaps were filled in the primary station using corresponding records from the other two nearby stations, see Table A1. If gaps remained, typically theses were no more than 10 consecutive hours, our team applied linear interpolation to estimate the missing values. This multi-step approach resulted in complete, gap-free meteorological datasets for each of the 13 wind farms. Ensuring data continuity at this stage was essential for enhancing the accuracy and reliability of subsequent modeling calculations, including wind speed adjustment, power output estimation, and curtailment impact analysis.

3.3 Wind farm performance calculation

To utilize the power curves (UL Solutions, 2024) of each turbine, the wind speeds from the completed datasets were adjusted to the hub heights of the turbines using a logarithmic wind profile equation (International Electrotechnical Commission, 2022), ensuring alignment with real operating conditions. The wind speed at hub height W_{hub} was calculated as Eq. (1):

$$W_{\text{hub}} = W_{\text{ref}} \frac{\ln(h_{\text{hub}}/z_0)}{\ln(h_{\text{ref}}/z_0)} \tag{1}$$

where: h_{ref} is the height at which wind speed measurements are originally recorded (10 m), W_{ref} is the measured wind speed at the reference height h_{ref}, h_{hub} is the turbine hub height, z_0 is the surface roughness length

Following this, CE-O calculated power output for each turbine by interpolating wind speeds along the turbine power curve. The power output at hub height was computed (International Electrotechnical Commission, 2022) as Eq. (2):

$$P = \left(P\left(W_{hub}\right) \times \left(\rho_{site}/\rho_{std}\right)^{1/3}\right) \times (1 - losses) \tag{2}$$

where: P is the estimated power output, $P\left(W_{hub}\right)$ is the turbine power curve function, ρ_{site} is the site-specific air density, ρ_{std} is the standard air density, $losses$ represent reductions in energy output due to turbine wake effects and general system inefficiencies.

In this study, the losses parameter in the Eq. (2), typically used to account for wake losses and system inefficiencies, was set to zero. This simplification was made to isolate the impact of curtailment strategies on energy production without introducing additional uncertainties from estimated system losses.

To obtain the final power output values, wind speeds at hub height were first adjusted for air density variations (Burton et al., 2021). The power curve function was then used to interpolate power output for each timestep using a linear interpolation method. This approach ensured that power output estimations reflected real-world operational conditions, including variations in air density and site-specific wind profiles (Burton et al., 2021).

Surface roughness values were determined using a land classification–based methodology. First, the distribution of land cover types within a 3 km radius of each wind turbine was assessed using the 2020 Land Cover of Canada dataset (Natural Resources Canada, 2020). The distributions from each wind turbine were then aggregated to form a distribution representative of the wind farm. Only the dominant land classification at each wind farm was selected to be used for calculations. Only two classification types covered the majority of the 13 analyzed wind farms, see Table A2, and were linked to their closest equivalents in the National Land Cover Database (NLCD), enabling the use of standardized seasonal roughness length values referenced in the U.S. Environmental Protection Agency's AERSURFACE tool (U.S. Environmental Protection Agency, 2020).

https://doi.org/10.5194/wes-2025-164
Preprint. Discussion started: 29 September 2025

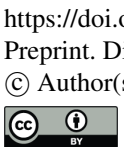

eawe european academy of wind energy
Open Access WIND ENERGY SCIENCE DISCUSSIONS

Figure 1 compares the total monthly power output of all turbines during July to September for the years 2020–2023, using AESO data as a reference alongside both the initial and the gap-filled modeled estimates. The results show that after applying the gap-filling process to the meteorological input data, the modeled outputs consistently aligned more closely with the AESO values.

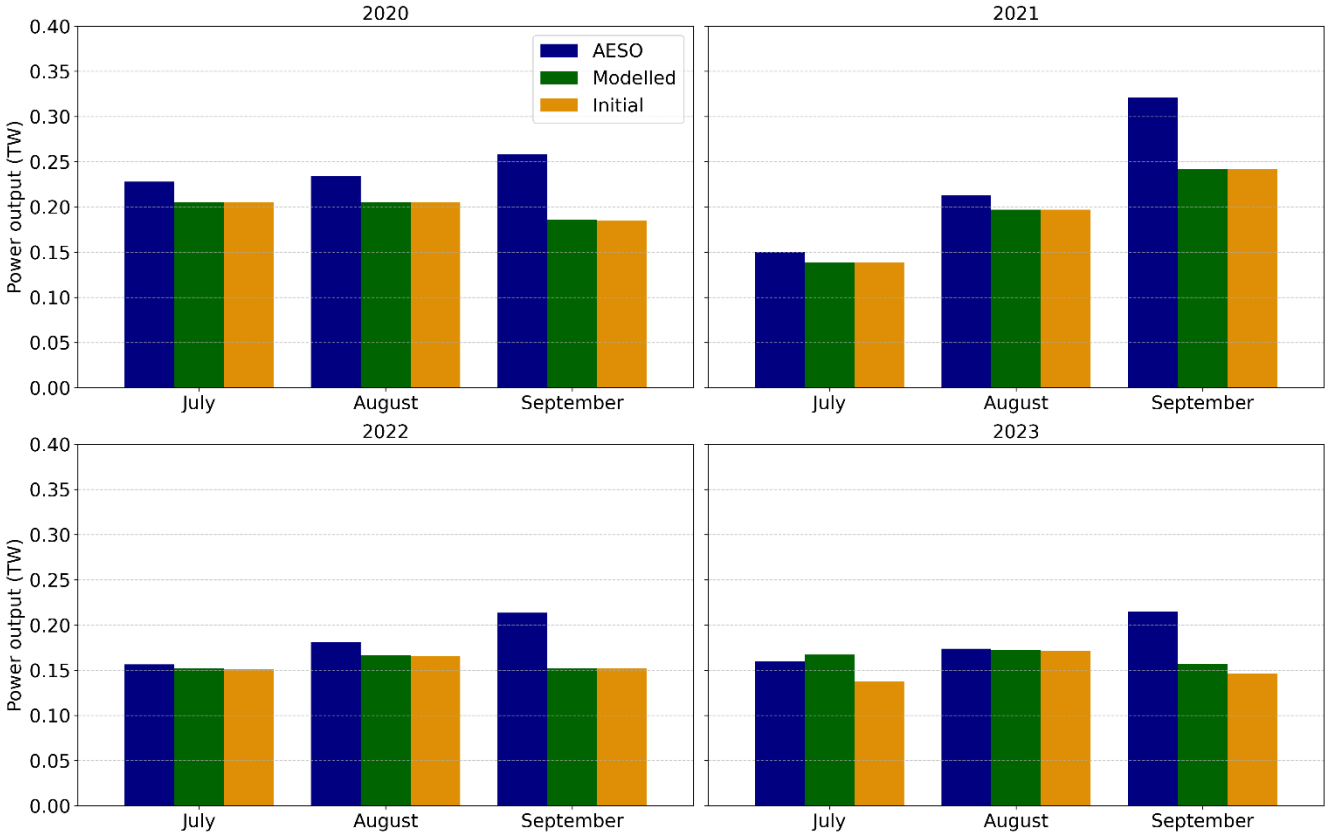

Figure 1. Annual power output comparison between observed (AESO), modeled, and initial estimates across all wind farms (2020–2023) during curtailed months.

3.4 Model validation

3.4.1 Quantitative Validation of Modeled Power Output

To validate our modeling results, CE-O compared the modeled power output with real generation data from the AESO, which served as a benchmark for evaluating the accuracy of our simulations. The comparison revealed a consistent improvement in model fidelity following the application of gap-filling techniques to the meteorological input data. In 2023, for example,

https://doi.org/10.5194/wes-2025-164
Preprint. Discussion started: 29 September 2025

eawe european academy of wind energy
Open Access WIND ENERGY SCIENCE DISCUSSIONS

the difference between the initial modeled output and AESO data was 25.01%, which was reduced to 19.36% after gap filling. Similar improvements were observed across the other years, with differences decreasing from 17.93% to 17.71% in 2020, from 17.73% to 17.69% in 2021, and from 16.60% to 14.53% in 2022. While the magnitude of improvement varied, the direction was consistent: gap-filled models more closely aligned with actual AESO power data in every year.

To assess the validity of the modeling approach and quantify its accuracy, CE-O compared the modeled wind power output to AESO's actual generation data using Mean Absolute Percentage Error (MAPE) and Root Mean Square Error (RMSE), following standard definitions (Montgomery et al., 2015), as shown in Eq. (3) and Eq. (4).

$$MAPE = \frac{100}{n} \sum_{i=1}^{n} \left| \frac{Forecast_i - Actual_i}{Actual_i} \right| \tag{3}$$

$$RMSE = \sqrt{\frac{1}{n} \sum_{i=1}^{n} (Forecast_i - Actual_i)^2} \tag{4}$$

where: i is the hourly time step, $Forecast_i$ is the modeled power output at each time step, $Actual_i$ is the real power output at each time step, n is the number of non-null observations.

The results indicate a modest improvement in model accuracy across all years, see Table A3. The Mean Absolute Percentage Error (MAPE) between modeled and observed AESO data was reduced from approximately 20.03% – 28.28% in the initial dataset to 18.41% – 24.06% after adjustments. Similarly, the Root Mean Square Error (RMSE) decreased from over 53,746 MW – 74,812 MW in the initial dataset to 47,965 MW – 62,320 MW in the final model — representing up to a 130% reduction in error, depending on the year. These results confirm that the applied gap-filling and calibration methods substantially increased the reliability of the modeled power output. The consistent improvements across all metrics and years highlight the importance of robust data correction and calibration practices to ensure that modeled datasets accurately reflect real-world wind power generation. These results highlight the importance of data corrections and calibration adjustments, ensuring that the final modeled dataset provides a more reliable representation of actual wind power generation.

3.4.2 Wind Speed Validation Using Backward Calculations

To independently validate the modeled hub-height wind speeds, the team performed a backward calculation using actual wind farm power output obtained from AESO and turbine-specific power curves. This process estimates the wind speed that would be required to produce the observed power generation.

First, turbine-level power output was derived by dividing the total farm-level output by the number of turbines at the site, as shown in Eq. (5):

$$P_T = \frac{P_F}{T_{Num}} \tag{5}$$

where: P_T is power output per turbine, P_F is power output per farm, T_{Num} is number of turbines.

https://doi.org/10.5194/wes-2025-164
Preprint. Discussion started: 29 September 2025

eawe european academy of wind energy
Open Access WIND ENERGY SCIENCE DISCUSSIONS

Wind speed was inferred using Eq. (6), where the turbine-level power output was adjusted for the site-specific air density, following the relationship:

$$P_T\left(W_{hub}\right) = \frac{P_T}{1-losses} \times \left(\frac{\rho_{std}}{\rho_{site}}\right)^{\frac{1}{3}} \tag{6}$$

In this study losses were set to zero.

The wind speed at hub-height W_{hub} was then obtained by inverting the turbine-specific power curves shown in Eq. (7):

$$P_T = \ P_T\left(W_{hub}\right) => \ W_{hub} = {P_T}^{-1}(P_T) \tag{7}$$

To minimize numerical instability and reduce the influence of flat or discontinuous regions of the power curve, the analysis was limited to wind speeds between 4 and 11 m/s, which correspond to the most sensitive portion of the turbine power curve with respect to the application of curtailment to reduce harm to bats. Values outside this range often produce unstable or flat regions, complicating back-calculations.

This method was applied across all turbines in the dataset, generating a time series of back-calculated wind speeds. These were then compared to the modeled wind speeds using distributional metrics. Figure 2 presents an example for a single wind farm, selected at random from the 13 sites in the study group, to illustrate the kernel density estimation comparison between modeled and back-calculated wind speeds.

https://doi.org/10.5194/wes-2025-164
Preprint. Discussion started: 29 September 2025

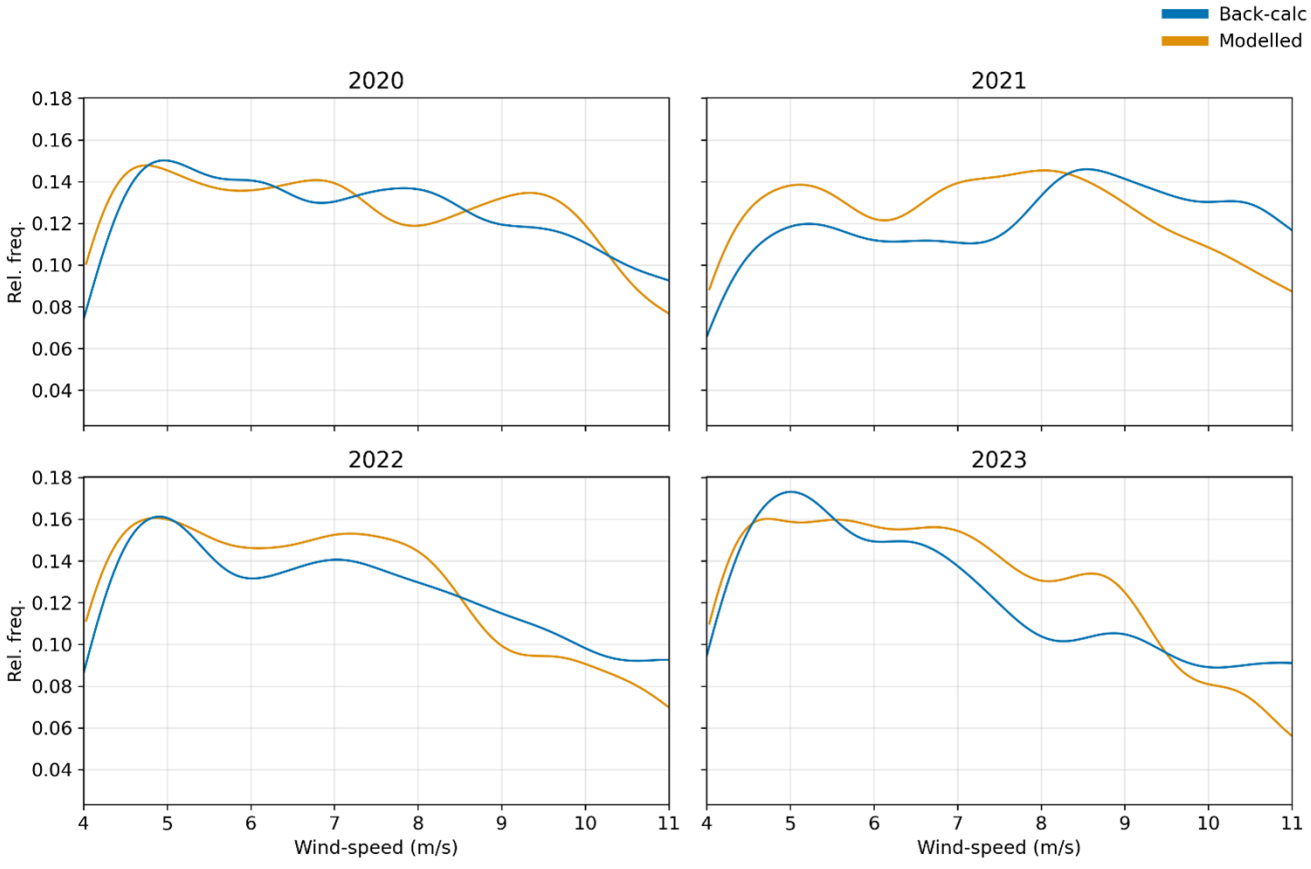

Figure 2. Example of kernel density estimation (KDE) of hub-height wind speed distributions for modeled versus back-calculated data across the period July 15 – September 30, for years 2020–2023.

To quantify how representative each weather station was for the wind conditions at its corresponding wind energy site, CE-O team compared the modeled wind-speed distributions to those derived from the backward-calculated approach. For each turbine and hub-height, wind speeds were binned into 4 – 11 m/s intervals, and the distributions from modeled and back-calculated data were normalized and compared using the root mean square error (RMSE). Then the RMSE was aggregated across years for each turbine and plotted against the distance from the associated ECCC weather station as shown on Figure 3. The resulting trend shows that while RMSE generally increases with distance, this relationship is not strictly linear. Notably, some sites at intermediate distances (20–30 km) exhibited higher RMSE than those located farther away, suggesting that proximity alone is not sufficient to ensure meteorological interrelation. These results underscore the importance of evaluating both spatial and climatic alignment when selecting reference stations for wind modeling.

https://doi.org/10.5194/wes-2025-164
Preprint. Discussion started: 29 September 2025

eawe european academy of wind energy
Open Access WIND ENERGY SCIENCE DISCUSSIONS

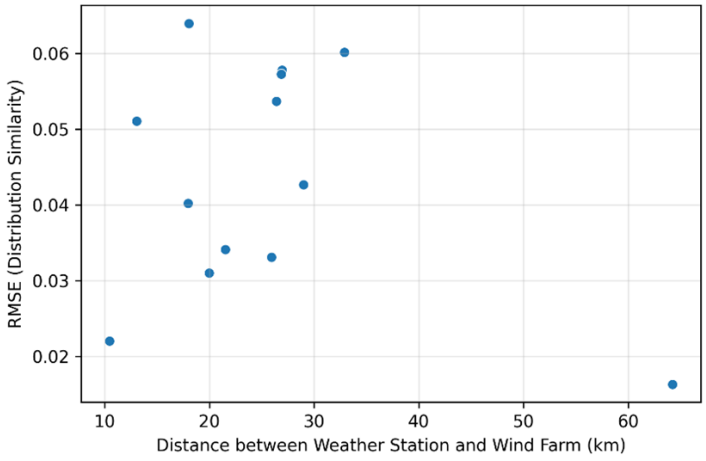

Figure 3. RMSE vs. Distance: Wind-speed Distribution Similarity (July 15 – Sep 30).

3.5 Estimating Financial Losses

To estimate the economic impact of curtailment strategies, hourly modeled energy losses (in MWh) were multiplied by the corresponding average pool price — the hourly market rate at which electricity is traded on Alberta's power grid. These prices were obtained from the AESO Annual Market Statistics Reports for the relevant years (Alberta Electric System Operator, 2024).

For each turbine and each curtailment scenario, the amount of curtailed energy was calculated at an hourly resolution during the specified curtailment windows. The resulting energy losses were then converted to revenue losses using the hourly average electricity price. This method provides a standardized estimate of financial impact that reflects Alberta's specific market conditions, with all values expressed in Canadian dollars (CAD).

In cases where hourly pool price data were missing, the gaps were filled with a value of zero. This conservative approach avoids artificially inflating loss estimates but may slightly underestimate total financial impacts if missing data coincided with periods of high electricity prices.

It is important to note that the economic loss estimates presented here account only for lost energy revenues and do not include the potential costs associated with implementing smart curtailment systems, such as meteorological sensors, control system integration, or ongoing maintenance.

4 Results

This section presents the key findings of the study, focusing on the impact of curtailment strategies on energy production and the associated economic losses. CE-O analyzed the differences in energy and financial losses under various curtailment scenarios,

https://doi.org/10.5194/wes-2025-164
Preprint. Discussion started: 29 September 2025

eawe european academy of wind energy
Open Access WIND ENERGY SCIENCE DISCUSSIONS

discussed interannual variations in losses, assessed the effect of increasing cut-in wind speeds, and examined interannual variations in outcomes.

Production, energy and economic losses were quantified for both blanket and smart curtailment strategies using wind speeds, power outputs and pool prices.

Energy losses were calculated using Eq. (8), which sums the difference between the power output P_t and the curtailed power output $P_{curtailet,t}$ at each time step:

$$L_{energy} = \sum_t (P_t - P_{curtailed,t}) \tag{8}$$

Economic losses were calculated using Eq. (9) by multiplying the curtailed energy at each time step by the corresponding pool price, $PoolPrice_t$, and summing over the analysis period:

$$L_{economic} = \sum_t (P_t - P_{curtailed,t}) \times PoolPrice_t \tag{9}$$

Finally, production losses in percentage terms were calculated using Eq. (10) as the ratio of total curtailed energy to total potential production (P_{annual}):

$$L_{production} = (\frac{L_{energy}}{P_{annual}}) \times 100 \tag{10}$$

Standard box-and-whisker plots were used to visualize the distribution of production and economic losses across all wind farms in the study group. Each box represents the interquartile range (IQR), spanning from the 25th percentile (Q1) to the 75th percentile (Q3) of the dataset. The line inside each box corresponds to the median (50th percentile), calculated using linear interpolation between the closest ranks (NumPy's Type 7 method), with quartiles defined in the same way (Hyndman and Fan, 1996).

The whiskers extend from the box to the most extreme values that lie within 1.5 × IQR from the lower and upper quartiles, respectively. Data points falling outside this range are considered statistical outliers and are plotted individually as separate markers. Outlier detection follows the Tukey rule, applied independently to each combination of season, year, cut-in speed, and curtailment strategy.

By structuring the plots this way, the figures convey both the central tendency and spread of the losses, while also highlighting atypical sites whose performance differs substantially from the broader group. From this point forward, when ranges are reported in the results, they represent the span from the lower to the upper whisker, exclude statistical outliers, and cover the entire four-year analysis period.

Figure 4 presents the annual production losses under different curtailment scenarios as a percentage of non-curtailed generation. Over all four years analyzed, smart curtailment reliably outperformed blanket curtailment in minimizing production losses. At a 5.5 m/s cut-in speed, blanket curtailment led to production losses ranging from 0.09% – 1.03%, while smart curtailment reduced losses to 0.05% – 0.63% depending on the year and curtailment scenario. At the highest cut-in speed of 8 m/s, production losses under blanket curtailment rose to 0.45% – 3.36%, while smart curtailment maintained lower losses between 0.42% and 2.40%.

https://doi.org/10.5194/wes-2025-164
Preprint. Discussion started: 29 September 2025

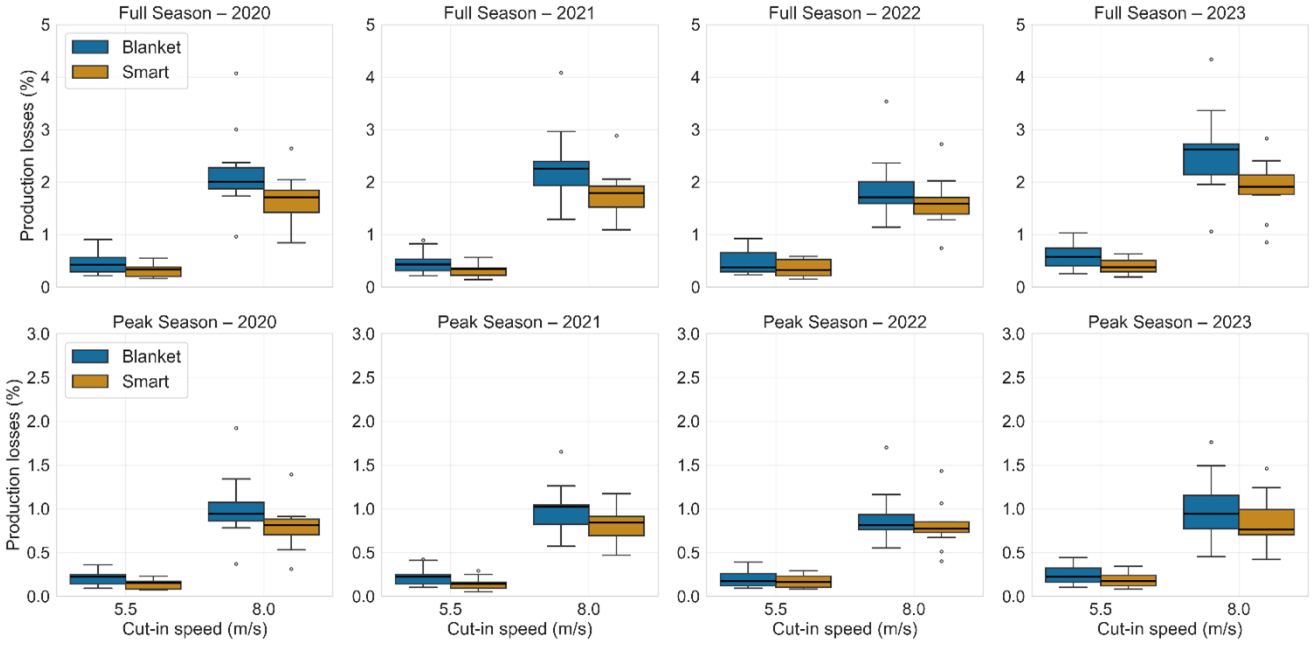

Figure 4. Annual production losses under different curtailment strategies (blanket vs. smart) and seasonal scenarios (full and peak seasons) for all wind farms (2020–2023).

Figure 5 presents the annual production losses derived from the backward-calculated hub-height wind speeds under different curtailment scenarios. Across all years, smart curtailment consistently resulted in lower production losses than blanket curtailment, mirroring the modeled calculation trends. At a 5.5 m/s cut-in speed, blanket curtailment led to production losses ranging from 0.05% to 0.5%, while smart curtailment reduced losses to 0.03% to 0.4%, depending on the year and curtailment scenario. At the highest analyzed cut-in speed of 8 m/s, production losses under blanket curtailment ranged from 0.2% to 3.8%, whereas smart curtailment maintained lower losses between 0.2% and 2.1%. These values are broadly consistent with the modeled results, reinforcing that the modeled and back-calculated wind speed datasets yield comparable curtailment impact estimates.

https://doi.org/10.5194/wes-2025-164
Preprint. Discussion started: 29 September 2025

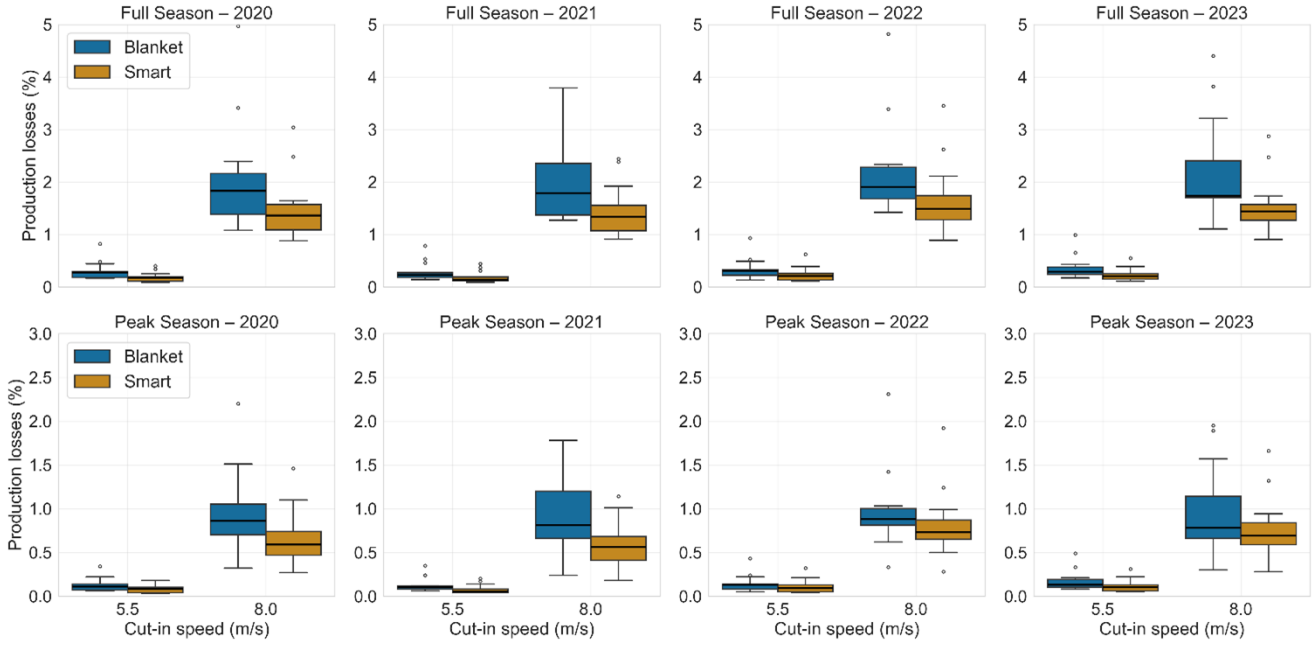

Figure 5. Annual production losses under blanket and smart curtailment strategies, derived from backward-calculated hub-height wind speeds, for full and peak seasons (2020–2023).

Figure 6 presents the annual normalized energy losses per megawatt of installed capacity under blanket and smart curtailment strategies for both the full and peak operational seasons from 2020 to 2023.

https://doi.org/10.5194/wes-2025-164
Preprint. Discussion started: 29 September 2025

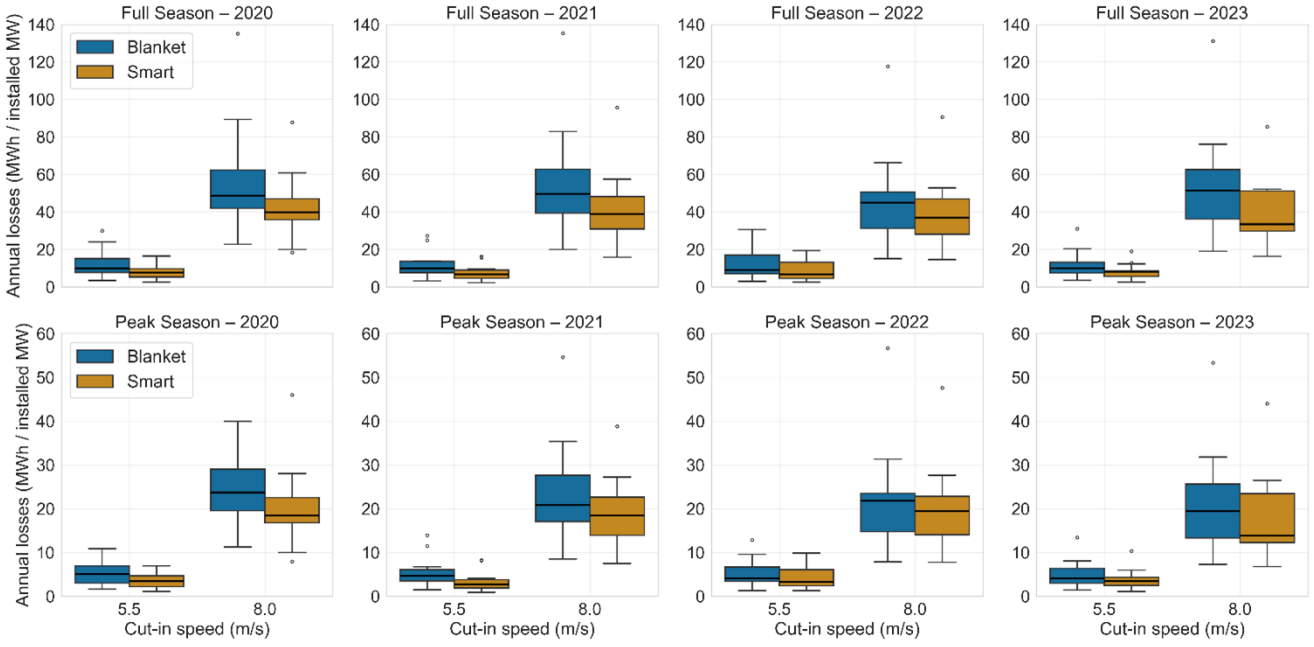

Figure 6. Annual power losses under different curtailment strategies (blanket vs. smart) and seasonal scenarios (full and peak seasons) for all wind farms (2020–2023).

Across all years, smart curtailment consistently reduced losses compared to blanket curtailment. At the lower cut-in threshold of 5.5 m/s, full-season losses ranged from 2.96 – 30.63 MWh/MW for blanket curtailment, compared to 2.24 – 19.37 MWh/MW for smart curtailment. In the peak season, losses at 5.5 m/s were lower overall, ranging from 1.27 – 10.85 MWh/MW for blanket curtailment and 0.89 – 9.82 MWh/MW for smart curtailment.

At the higher cut-in threshold of 8.0 m/s, losses increased sharply for both strategies. Full Season blanket curtailment caused losses of 15.03 – 89.34 MWh/MW, compared to 14.52 – 60.86 MWh/MW with smart curtailment. In the Peak Season, the range narrowed to 7.28 – 39.96 MWh/MW for blanket curtailment and 6.77 – 28.04 MWh/MW for smart curtailment.

Overall, smart curtailment reduced energy losses by approximately 3 – 37% depending on season and cut-in speed, with the largest savings observed at 5.5 m/s during the full season (24 – 37% reduction) and the smallest at 8.0 m/s during the full season (3%).

In addition to energy losses, corresponding financial impacts were estimated for both blanket and smart curtailment strategies. At a 5.5 m/s cut-in speed in the full season, annual financial losses ranged from $125 – $4,000 CAD/installed MW under blanket curtailment but were reduced to $100 – $3,000 CAD/installed MW under smart curtailment. At the higher 8.0 m/s cut-in speed, losses increased substantially, reaching $685 – $11,760 CAD/installed MW for blanket curtailment compared to $596 – $10,130 CAD/installed MW for smart curtailment.

https://doi.org/10.5194/wes-2025-164
Preprint. Discussion started: 29 September 2025

eawe european academy of wind energy
Open Access WIND ENERGY SCIENCE DISCUSSIONS

In the peak season, financial losses were generally lower than in the full season but still showed clear savings from smart curtailment. At a 5.5 m/s cut-in speed, blanket curtailment led to annual financial losses ranging from $50 – $2,366 CAD/installed MW, while smart curtailment reduced this range to $35 – $2,000 CAD/installed MW.

At the higher cut-in threshold of 8.0 m/s, losses increased to $293 – $5,152 CAD/installed MW under blanket curtailment, compared to $222 – $4,800 CAD/installed MW with smart curtailment.

These differences illustrate that even during the peak season, when bat activity and curtailment measures are concentrated, smart curtailment can substantially reduce financial impacts compared to a blanket approach.

Figure 7 illustrates the relationship between production losses and cut-in wind speed under different curtailment strategies across all wind farms in the study group. For each cut-in speed and curtailment strategy, losses were aggregated by summing the total curtailed production (in MWh) across all sites and dividing by the total non-curtailed production across the same sites and period, yielding a fleet-wide percentage loss. The results show that production losses increase significantly with higher cut-in speeds, with blanket curtailment showing the highest losses in all scenarios. Smart curtailment consistently results in 27 – 36% lower production losses in the full season and 20 – 33% lower losses in the peak season compared to blanket curtailment, highlighting its effectiveness in minimizing energy losses.

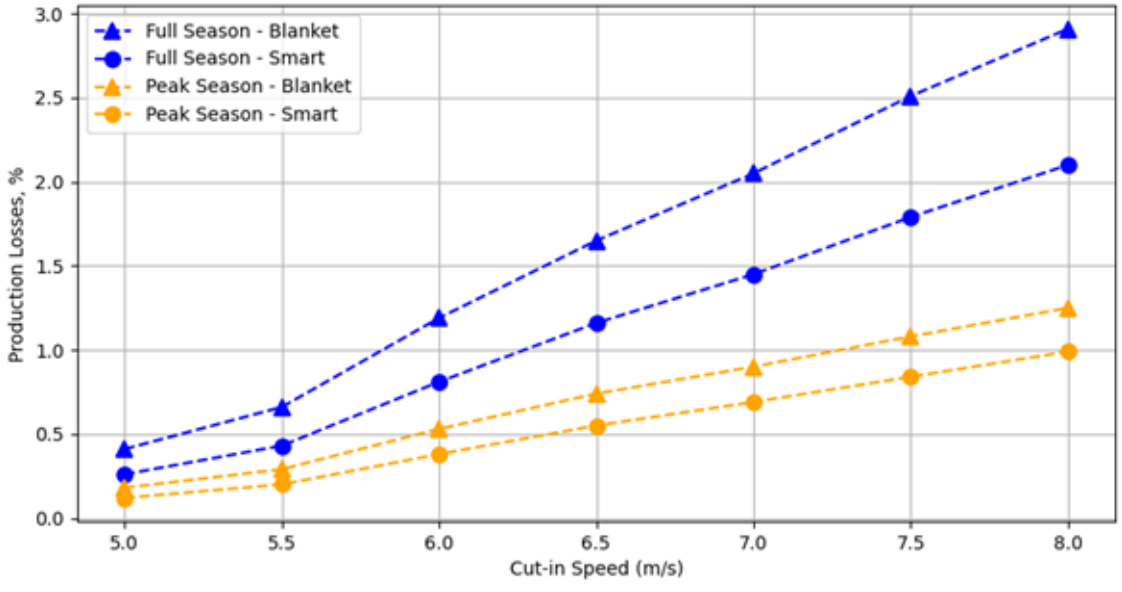

Figure 7. Percentage increase in production losses when increasing cut-in wind speed from 5.5 m/s to 8.0 m/s, across all years, scenarios, and curtailment strategies.

https://doi.org/10.5194/wes-2025-164
Preprint. Discussion started: 29 September 2025

eawe european academy of wind energy
Open Access WIND ENERGY SCIENCE DISCUSSIONS

5 Conclusions

Overall, this study highlights the critical role of curtailment strategies in shaping wind energy production and associated economic outcomes. The accuracy of our modeled wind power data played a crucial role in these findings. The improvements in model precision, achieved through gap-filling, enhanced the alignment between modeled and real power output. The reduction in MAPE and RMSE values confirms a closer alignment between the modeled and observed data, improving confidence in the dataset's suitability for evaluating curtailment scenarios.

Across all years and cut-in thresholds, smart curtailment consistently reduced energy and economic losses by 3 – 36% compared to blanket curtailment. Shortening the curtailment window from July 15 – September 30 to August 1 – September 10 resulted in 7 – 30% lower annual losses, depending on the year and wind speed threshold. Interannual variation was also significant: 2022, a high-wind year, had the highest overall curtailment losses. However, the percentage difference between 5.5 m/s and 8.0 m/s cut-in thresholds was greatest in 2020, a low-wind year, where using the lower threshold reduced losses by up to 80%. These trends demonstrate how seasonal wind conditions strongly influence curtailment impacts. While this study did not assess bat mortality directly, prior research has shown that shorter curtailment periods may increase risk to bats depending on migration timing (e.g., Arnett et al., 2016). Further ecological modeling would be needed to evaluate the trade-offs between energy conservation and species protection.

The results allow us to approximate potential power and financial losses under different curtailment scenarios and operational strategies. The increase in losses associated with higher cut-in wind speeds underscores the importance of carefully evaluating operational decisions. These findings offer valuable insights for policymakers and industry stakeholders aiming to balance energy efficiency with environmental considerations.

https://doi.org/10.5194/wes-2025-164
Preprint. Discussion started: 29 September 2025

eawe european academy of wind energy
Open Access WIND ENERGY SCIENCE DISCUSSIONS

Table A1: List of the three nearest meteorological stations to each wind farm site, including their distances used for data gap filling.

Asset name	Nearby station	Distance (km)
Ardenville	Blood Tribe AGDM	27
Ardenville	Fort Macleod AGCM	27
Ardenville	Glenwood	25
Blackspring Ridge	Barons AGCM	26
Blackspring Ridge	Iron Springs AGDM	27
Blackspring Ridge	Travers AGCM	20
Blue Trail Wind	Cardston	54
Blue Trail Wind	Fort Macleod AGCM	16
Blue Trail Wind	Waterton Park Gate	64
ARM2262 Castle River	Beaver Mines	10
ARM2262 Castle River	Glenwood	43
ARM2262 Castle River	Stavely AAFC	76
Enel Alberta Castle Rock	Beaver Mines	18
Enel Alberta Castle Rock	Glenwood	45
Enel Alberta Castle Rock	Stavely AAFC	67
Magrath	Blood Tribe AGDM	22
Magrath	Raymond AGDM	22
Magrath	St. Mary Reservoir	12
Halkirk Wind Power Facility	Alliance AGCM	20
Halkirk Wind Power Facility	Forestburg AGCM	32
Halkirk Wind Power Facility	Halkirk AGCM	18
Summerview 1	Beaver Mines	33
Summerview 1	Glenwood	36
Summerview 1	Stavely AAFC	64
Kettles Hill Wind	Beaver Mines	27
Kettles Hill Wind	Glenwood	29
Kettles Hill Wind	Stavely AAFC	74
Oldman 2 Wind Farm	Beaver Mines	26
Oldman 2 Wind Farm	Glenwood	36
Oldman 2 Wind Farm	Stavely AAFC	67
Suncor Chin Chute	Barnwell AGDM	13
Suncor Chin Chute	Raymond AGDM	35
Suncor Chin Chute	Wrentham AGDM	25

https://doi.org/10.5194/wes-2025-164
Preprint. Discussion started: 29 September 2025

eawe european academy of wind energy
Open Access WIND ENERGY SCIENCE DISCUSSIONS

Table A1: List of the three nearest meteorological stations (continued)

Asset name	**Nearby station**	**Distance (km)**
Enmax Taber	Fincastle AGDM	8
Enmax Taber	Foremost AGDM	45
Enmax Taber	Wrentham AGDM	29
Ghost Pine	Delburne AGCM	33
Ghost Pine	Three Hills	18
Ghost Pine	Wimborne AGCM	16

https://doi.org/10.5194/wes-2025-164
Preprint. Discussion started: 29 September 2025

eawe european academy of wind energy
Open Access WIND ENERGY SCIENCE DISCUSSIONS

Table A2. Land classification values and descriptions for each wind farm.

Wind farm	CLC value	CLC description	NLCD value	NLCD description
Ardenville	10	Temperate or sub-polar grassland	71	Grasslands/Herbaceous
ARM2262 Castle River	15	Cropland	82	Row Crops
Blackspring Ridge	15	Cropland	82	Row Crops
Blue Trail Wind	10	Temperate or sub-polar grassland	71	Grasslands/Herbaceous
Enel Alberta Castle Rock	15	Cropland	82	Row Crops
Enmax Taber	15	Cropland	82	Row Crops
Ghost Pine	15	Cropland	82	Row Crops
Halkirk Wind Power Facility	15	Cropland	82	Row Crops
Kettles Hill Wind	15	Cropland	82	Row Crops
Magrath	15	Cropland	82	Row Crops
Oldman 2 Wind Farm	10	Temperate or sub-polar grassland	71	Grasslands/Herbaceous
Summerview 1	15	Cropland	82	Row Crops
Suncor Chin Chute	15	Cropland	82	Row Crops

CLC = Canada Land Cover; NLCD = National Land Cover Database.

https://doi.org/10.5194/wes-2025-164
Preprint. Discussion started: 29 September 2025

eawe european academy of wind energy
Open Access WIND ENERGY SCIENCE DISCUSSIONS

Table A3. MAPE and RMSE values for both the modeled and initial datasets compared to AESO across the years.

Year	Comparison	MAPE (%)	RMSE (MW)
2020	Modeled vs AESO	19.78	62 320.38
2020	Initial vs AESO	20.03	62 538.97
2021	Modeled vs AESO	19.47	61 099.09
2021	Initial vs AESO	19.53	61 191.02
2022	Modeled vs AESO	18.41	47 964.50
2022	Initial vs AESO	19.74	53 746.22
2023	Modeled vs AESO	24.06	56 062.98
2023	Initial vs AESO	28.28	74 811.76

https://doi.org/10.5194/wes-2025-164
Preprint. Discussion started: 29 September 2025

eawe european academy of wind energy
Open Access WIND ENERGY SCIENCE DISCUSSIONS

Code availability. The code used to generate curtailment scenarios and reproduce the analyses presented in this paper is publicly available under an open-source license via the GitHub–Zenodo integration: curtailment_scenarios (tag v1.0.0), https://doi.org/10.5281/zenodo.16995974.

Data availability. All datasets used in this study are archived on Zenodo: https://doi.org/10.5281/zenodo.16996187.

Author contributions. AS, RK, and IM designed the analysis and developed the methodology. AS developed the code, performed the simulations, and prepared the manuscript with contributions from all co-authors. IM verified the calculations and results. KL conducted the technical review, including proposing revisions to the methodology.

Competing interests. The authors declare that they have no conflict of interest.

Financial support. This work was supported by the Program for Energy Research and Development at Natural Resources Canada https://natural-resources.canada.ca/funding-partnerships/program-energy-research-development.

Acknowledgements. The authors thank Michael Sullivan and Karim Valji for sharing ideas and providing reciprocal feedback. We acknowledge Environment and Climate Change Canada (ECCC) for meteorological observations and the Alberta Electric System Operator (AESO, 2024) for operational and market data used in this study.

https://doi.org/10.5194/wes-2025-164
Preprint. Discussion started: 29 September 2025

eawe european academy of wind energy
Open Access WIND ENERGY SCIENCE DISCUSSIONS

References

Alberta Electric System Operator: Energy Trading System (ETS) Portal, http://ets.aeso.ca/, (last access: August 2025), 2024.

Alberta Environment and Sustainable Resource Development: Bat Mitigation Framework for Wind Power Development, Tech. rep., Government of Alberta, Edmonton, Canada, https://open.alberta.ca/publications/bat-mitigation-framework-for-wind-power-development, 2013.

Arnett, E. B., Baerwald, E. F., Mathews, F., Rodrigues, L., Rodríguez-Durán, A., Rydell, J., and Voigt, C. C.: Impacts of wind energy development on bats: a global perspective, in: Bats in the Anthropocene: Conservation of Bats in a Changing World, edited by Voigt, C. C. and Kingston, T., pp. 295–323, Springer, Cham, https://doi.org/10.1007/978-3-319-25220-9_11, 2016.

Burton, T., Sharpe, D., Jenkins, N., and Bossanyi, E.: Wind Energy Handbook, Wiley, Chichester, UK, 3 edn., https://doi.org/10.1002/9781119992714, 2021.

Canadian Renewable Energy Association: By the Numbers, https://renewablesassociation.ca/by-the-numbers/, (last access: August 2025), 2024.

Environment and Climate Change Canada: Historical Climate Data, https://climate.weather.gc.ca/, (last access: August 2025), 2024.

Frick, W. F., Baerwald, E. F., Lintott, P. R., McGuire, L. P., Barclay, R. M. R., and Voigt, C. C.: Bats and wind energy: mortality, mitigation, and future directions, Ann. N. Y. Acad. Sci., 1508, 158–173, https://doi.org/10.1111/nyas.15225, 2023.

Hyndman, R. J. and Fan, Y.: Sample Quantiles in Statistical Packages, The American Statistician, 50, 361–365, https://doi.org/10.2307/2684934, 1996.

International Electrotechnical Commission: Wind energy generation systems – Part 12-1: Power performance measurements of electricity producing wind turbines, Tech. Rep. IEC 61400-12-1:2022, IEC, Geneva, Switzerland, https://webstore.iec.ch/en/publication/69211, 2022.

International Energy Agency: Renewables 2024, https://www.iea.org/reports/renewables-2024, 2024.

Maclaurin, G., Hein, C., Williams, T., Roberts, O., Lantz, E., Buster, G., and Lopez, A.: National-scale impacts on wind energy production under curtailment scenarios to reduce bat fatalities, Wind Energy, 25, https://doi.org/10.1002/we.2741, 2022.

Montgomery, D. C., Jennings, C. L., and Kulahci, M.: Introduction to Time Series Analysis and Forecasting, Wiley, Hoboken, NJ, USA, 2 edn., ISBN 9781118745113, chapter 2, 2015.

Natural Resources Canada: Land Cover of Canada, https://search.open.canada.ca/openmap/ee1580ab-a23d-4f86-a09b-79763677eb47, (last access: August 2025), 2020.

Natural Resources Canada: Canadian Wind Turbine Database (CWTDB) — Open Government Portal, https://open.canada.ca/data/en/dataset/79fdad93-9025-49ad-ba16-c26d718cc070, (last access: August 2025), 2024.

Ontario Ministry of Natural Resources and Forestry: Bats and Bat Habitats: Guidelines for Wind Power Projects, https://www.ontario.ca/document/bats-and-bat-habitats-guidelines-wind-power-projects, 2011.

Ontario Ministry of the Environment, Conservation and Parks: The Committee on the Status of Species at Risk in Ontario's 2023 Annual Report, https://ero.ontario.ca/notice/019-8295, 2024.

Ontario Ministry of the Environment, Conservation and Parks: Amendments to the Species at Risk in Ontario List in response to COSSARO's 2023 Annual Report, https://ero.ontario.ca/notice/019-9436, 2025.

Thurber, B. G., Kilpatrick, R. J., Tang, G. H., Wakim, C., and Zimmerling, J. R.: Economic Impacts of Curtailing Wind Turbine Operations for the Protection of Bat Populations in Ontario, Wind, 3, 291–301, https://doi.org/10.3390/wind3030017, 2023.

https://doi.org/10.5194/wes-2025-164
Preprint. Discussion started: 29 September 2025

330 UL Solutions: Windographer – Wind Data Analytics and Visualization Solution, https://www.ul.com/software/windographer-wind-data-analytics-and-visualization-solution, (last access: August 2025), 2024.

U.S. Environmental Protection Agency: AERSURFACE User's Guide (Version 20060), Tech. rep., Office of Air Quality Planning and Standards, Air Quality Modeling Group, https://www.epa.gov/sites/default/files/2020-09/documents/aersurface_userguide.pdf, 2020.